ACS OMEGA

http://pubs.acs.org/journal/acsodf

Article

Comparison of Attachment and Antibacterial Activity of Covalent and Noncovalent Lysozyme-Functionalized Single-Walled Carbon Nanotubes

Matthew M. Noor, Joyanta Goswami, and Virginia A. Davis*

Cite This: *ACS Omega* 2020, 5, 2254−2259

Read Online

ACCESS | Metrics & More | Article Recommendations

ABSTRACT: Carbon nanotube−lysozyme (LSZ) conjugates provide an attractive combination of high strength and antimicrobial activity. However, there has not been a direct comparison of the covalent and noncovalent methods for creating them. In this work, single-walled carbon nanotubes (SWNT) were functionalized with LSZ using both noncovalent adsorption and covalent attachment via *N*-ethyl-*N*-(3-dimethylamino-propyl) carbodiimide hydrochloride−*N*-hydroxysuccinimide (EDC−NHS) chemistry. The amount of attached lysozyme, dispersion stability, and antimicrobial activity was compared. In addition, the mechanical properties of LSZ−SWNT in poly(vinyl alcohol) (PVA) composite films were investigated. Dispersions of covalently bound LSZ−SWNT had better dispersion stability. This was attributed to covalent functionalization enabling sustained SWNT dispersion at a lower LSZ/SWNT ratio. The covalently bound LSZ−SWNT also exhibited a lower initial rate of antibacterial response but were active over a longer time scale. Composite films made from LSZ−SWNT maintained similar activity as the corresponding dispersions. However, the noncovalent LSZ−SWNT films were stronger and more hydrolytically stable than those made from covalent LSZ−SWNT.

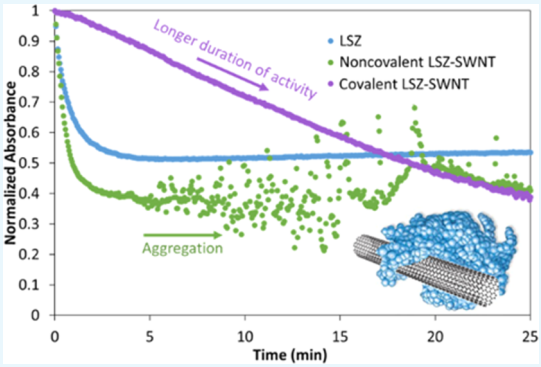

INTRODUCTION

In recent years, research on the combination of carbon nanomaterials with proteins and enzymes has been driven by two desires: (1) enabling aqueous dispersions and (2) combining carbon nanomaterials' electrical, mechanical, thermal, or optical properties with those inherent in biological materials.[1−7] Adducts of lysozyme (LSZ) and carbon nanomaterial have attracted particular interest due to the enzyme's natural abundance, inherent antibacterial activity, and stability. In addition, both experimental and computational investigations have shown that lysozyme's tryptophan residue has favorable interactions with sp^2-hybridized carbon nanomaterials. These interactions enable dispersion of single-walled carbon nanotubes (SWNT),[2,8−11] multiwalled carbon nanotubes (MWNT),[12] graphene oxide,[13] and fullerenes such as C_{60}[14,15] at higher concentrations than can be achieved with many other biological or synthetic dispersion aids. LSZ−carbon nanomaterial dispersions have been used to produce antimicrobial carbon nanotube films and fibers[16,17] and sort nanotubes by size.[18]

While much of the research has focused on attaching LSZ to carbon nanomaterials via noncovalent interactions, this approach does have some disadvantages. For SWNT, efforts to increase the concentration of LSZ−SWNT dispersions result in depletion attraction and nanotube aggregation above 0.15 vol% SWNT at a 2.1:1.0 LSZ:SWNT ratio.[16] Therefore, achieving higher concentrations more suitable for film or fiber production requires a different approach. Horn et al. added both a surfactant and a polymer to create dispersions with higher SWNT concentration, which could be dry-spun into antimicrobial fibers with toughnesses greater than spider silk.[16] Similarly, Nyankima et al. used a poly(vinyl alcohol) (PVA) solution to produce transparent antimicrobial films.[17] In contrast, Merli et al. demonstrated that LSZ could be covalently attached to multiwalled carbon nanotubes (MWNT) using standard *N*-ethyl-*N*-(3-dimethylamino-propyl) carbodiimide hydrochloride−*N*-hydroxysuccinimide (EDC−NHS) chemistry; this approach resulted in greater antimicrobial activity than native LSZ.[19] To date, there has not been a direct comparison of covalently and noncovalently functionalized LSZ−SWNT adducts. This paper reports a comparison of the two functionalization methods using spectroscopic and thermal gravimetric characterization and turbidimetric assays for antibacterial activity. In addition, a

Received: October 11, 2019
Accepted: January 14, 2020
Published: January 27, 2020

https://dx.doi.org/10.1021/acsomega.9b03387
ACS Omega 2020, 5, 2254−2259

comparison of antibacterial and mechanical properties of composite LSZ−SWNT−PVA films made from the dispersions is reported.

RESULTS AND DISCUSSION

Differences between covalently and noncovalently functionalized LSZ−SWNT were evaluated in terms of relative dispersion concentrations, differences in interactions based on Fourier transform infrared (FTIR) spectra, supernatant antimicrobial activity, and the antimicrobial activity and mechanical properties of LSZ−SWNT−PVA films. The noncovalently functionalized LSZ−SWNT were prepared and characterized using previously established methods.[8,16,17] Covalent attachment was performed using EDC−NHS chemistry following the method developed by Merli et al. for LSZ functionalization of MWNT.[19] The LSZ and SWNT concentrations for noncovalent functionalization were chosen for consistency with the previous work.[17] The concentration of the covalently functionalized LSZ−SWNT was chosen to be consistent with SWNT concentration in noncovalent LSZ−SWNT dispersions (e.g., 1 mg/mL covalent LSZ−SWNT).

Comparison of Attachment Methods. The initial dispersions from each method are referred to as mixtures in the remainder of this manuscript. Centrifugation of each mixture at 17 000*g* for 3 h resulted in supernatants, which contained individual LSZ−SWNT and small LSZ−SWNT bundles. Supernatants of noncovalently functionalized LSZ−SWNT also contained free LSZ. As described in Materials and Methods, the concentrations of each component in the supernatants and amount of bound LSZ were determined using a combination of UV−vis spectroscopy and thermal gravimetric analysis, based on previously reported methods.[8,16,17] These results are shown in Table 1. Repeated washing of the noncovalently functionalized samples showed that only 18−25% of the total LSZ was bound to the SWNT. However, as anticipated, rinsing the covalently functionalized LSZ did not reveal any free LSZ. Interestingly, while the initial LSZ/SWNT ratio (by mass) was higher for the noncovalent dispersion, fewer LSZ molecules were bound per SWNT than in the covalent functionalization.

Table 1. Relative Amounts of LSZ and SWNT in Mixtures and Supernatants of Noncovalently and Covalently Functionalized LSZ−SWNT

	noncovalent LSZ−SWNT		covalent LSZ−SWNT	
	mixture	supernatant	mixture	supernatant
SWNT (mg/mL)	1.0	0.69	0.21	0.14
LSZ_{total} (g/mL)	5.0	3.8	0.79	0.25
LSZ_{bound} (mg/mL)	0.89	0.97	0.79	0.25
LSZ_{total}/SWNT (mass)	5.0	5.5	3.8	1.8
LSZ_{bound}/SWNT (mass)	0.89	1.4	3.8	1.8
LSZ_{bound}/SWNT (number)	30	57	100	60
SWNT carbons per bound LSZ	1300	660	280	470

Since covalent functionalization results in the conversion of sp^2- to sp^3-hybridized carbon, Raman spectroscopy was used to verify covalent attachment. The G band located at 1592 cm^{-1} is due to tangential stretching of sp^2-hybridized carbon, while the D band located at 1356 cm^{-1} is due to tangential stretching of sp^3-hybridized carbon. Therefore, the ratio of the intensities of the D and G peaks is a facile way to verify covalent functionalization.[20] Figure 1a shows the Raman spectra for the pristine SWNT, noncovalently functionalized LSZ−SWNT, and covalently functionalized LSZ−SWNT using a 514 nm laser. The D/G ratios for the pristine and noncovalently functionalized SWNT were within the experimental error with average values of 0.11 and 0.08, respectively. For the covalent LSZ−SWNT, the D/G ratio increased to 0.22 consistent with covalent functionalization.

FTIR provided insights into the effects of SWNT attachment on LSZ. Comparing the position, relative intensity, and shape of a protein's amide I and amide II bands are one of the key methods for identifying protein−nanomaterial interactions and protein conformational changes.[8] The amide I band is primarily due to C═O stretching of the peptide, while the amide II peak is primarily due to C−N stretching as well as N−H bending. Figure 1b shows FTIR spectra of the covalent and noncovalent LSZ−SWNT supernatants and LSZ prepared by an equivalent method without the addition of SWNT. For the pure LSZ dispersion, the amide I band was symmetric, centered at 1651 cm^{-1}, and had approximately twice the intensity as the symmetric amide II band centered at 1533 cm^{-1}. In the case of noncovalent SWNT functionalization, the amide I band was similar to that for pure LSZ, centered at 1650 cm^{-1}. This indicates that interaction with the SWNT had little effect on the LSZ backbone's secondary structure.[21] However, the amide I band for the noncovalently functionalized LSZ−SWNT had nearly four times the intensity of the amide II band and was significantly downshifted to 1526 cm^{-1}. Furthermore, the increased intensity of the amide III bands (1200−1350 cm^{-1}) indicates significant changes to LSZ's secondary and tertiary structures. It has been established in the literature that sonication of aqueous LSZ−SWNT dispersions results in the simultaneous debundling of SWNT and partial unfolding of LSZ; this exposes the tryptophan residue, which then experiences $\pi-\pi$ interactions with SWNT.[1,2,8,12] Cessation of sonication results in the refolding of LSZ, but the presence of the SWNT inhibits restoration of the original conformation. In contrast, covalent functionalization through EDC−NHS chemistry resulted in a similar amide I to amide II intensity ratio and amide III peaks as the pure LSZ. However, the covalent functionalization resulted in a greater downshift in the amide I band to 1648 cm^{-1} suggesting more changes to the LSZ backbone, but less shift in the amide II band, which was centered at 1531 cm^{-1}.

In addition to determining the relative amounts of bound components, thermogravimetric analysis (TGA) also provided insight into the thermal stability resulting from the two functionalization methods. In an inert argon atmosphere, Figure 2a, the thermal stabilities of both covalent and noncovalent LSZ−SWNT are similar until 560 °C. After 560 °C, the difference in thermal stability is due to oxidation and subsequent covalent functionalization causing a loss in the thermal stability of the SWNT. The TGA curves in the air atmosphere, Figure 2b, show higher thermal stability for the covalent sample and lower thermal stability for the noncovalent sample compared to both the SWNT and LSZ curves. It can be inferred that covalent functionalization has some stabilization effect on the LSZ, while the slight denaturation of LSZ during sonication was most likely the cause of lowered thermal stability of the noncovalent LSZ−SWNT sample.

Comparison of Dispersion Antimicrobial Activity. The effects of the type of functionalization on the LSZ's

https://dx.doi.org/10.1021/acsomega.9b03387
ACS Omega 2020, 5, 2254−2259

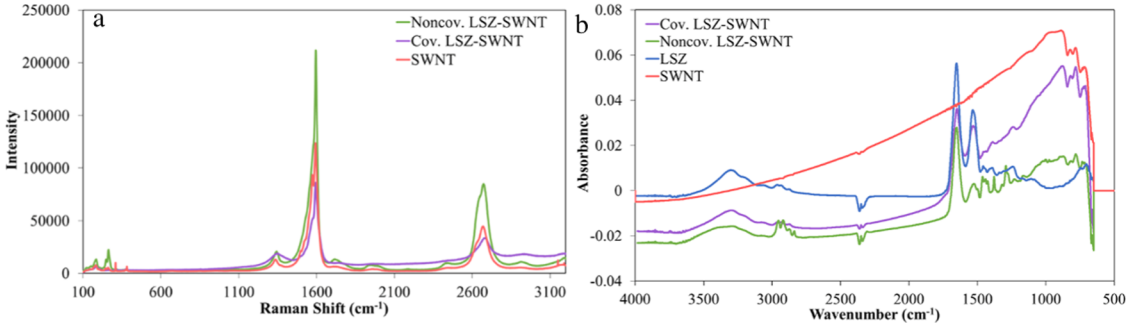

Figure 1. Spectroscopic characterization. (a) Raman Spectra performed with a 514 nm laser of SWNT and both covalent and noncovalent LSZ−SWNT. (b) FTIR spectra of covalent and noncovalent bonded SWNT−LSZ as well as SWNT and native LSZ.

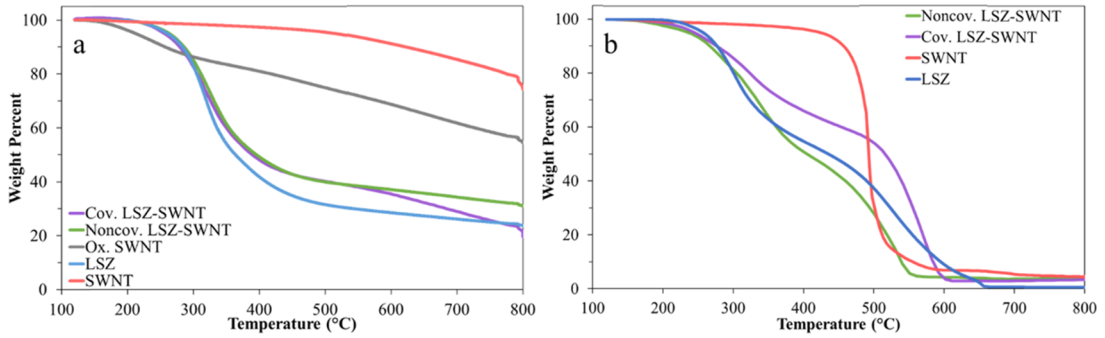

Figure 2. Representative TGA plots in (a) argon and (b) air atmospheres.

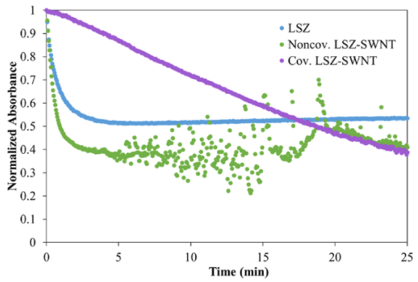

	LSZ	Noncov. LSZ-SWNT	Covalent LSZ-SWNT
Linear cell death slope	0.66	0.94	0.02
Specific activity (active units/mg LSZ)	1977	1586	1295
Native LSZ activity maintained (%)	100	80	66

Figure 3. Turbidimetric assay of dispersions as well as a table showing initial cell death slope, specific activity, and percentage of native LSZ activity maintained for each dispersion.

antimicrobial activity were compared using the standard assay recommended by the supplier;[22] this method was chosen for consistency with the previous work.[8,16,17,23] This UV−vis spectroscopy method is based on changes in turbidity resulting from the lysis of *Micrococcus lysodeikticus*, measured at 450 nm and normalized by the initial absorbance

$$\text{activity} = \frac{(\Delta \text{Abs}_{450}/t)_{\text{test}} - (\Delta \text{Abs}_{450}/t)_{\text{blank}}}{0.001(m)_{\text{LSZ}}} \quad (1)$$

where ΔAbs_{450} is the change in the 450 nm absorbance intensity, t is the test duration, m_{LSZ} is the mass of LSZ, and the test or blank indicates the dispersion or buffer solution. Only supernatants were used in these assays so that only individual or small bundles of SWNT were present. Since the goal of the research was to compare the results of the two functionalization methods, no efforts were made to remove free lysozyme from the noncovalent supernatants. As shown in Figure 3, the native LSZ showed an immediate decrease in absorbance that initially followed the Michaelis−Menten kinetics, and then plateaued after approximately 5 min. Similar behavior was exhibited by the noncovalent LSZ−SWNT, but the initial activity (decrease in absorbance) was more significant, and after 5 min, the data became scattered due to the formation of SWNT flocs, which intermittently obscured the optical path. In contrast, covalent SWNT−LSZ showed a continuous, nearly linear decrease in absorbance throughout the measurement time. The 80% maintained activity of noncovalent LSZ−SWNT is in agreement with the results of Horn et al.[8]

The linear cell death slope or initial rates of lysis activity of the SWNT−LSZ and LSZ dispersions are shown in Figure 3. They were obtained by finding the natural logarithm of the first 0.5 min in the initial linear region of the native LSZ and SWNT−LSZ dispersions and obtaining the corresponding slopes.[17] The noncovalent SWNT−LSZ had a higher activity rate of 0.93 min^{-1} compared to the native LSZ rate of 0.57 min^{-1}. Covalently bound SWNT−LSZ had a much lower rate of 0.014 min^{-1}, but retained its activity over a much longer period. This combined with the absence of flocculation over the assay period suggests stabilization of the SWNT dispersion state by covalent LSZ functionalization. However, in contrast to investigations by Merli et al. of covalent LSZ-MWNT functionalization, the data do not indicate that the presence of

https://dx.doi.org/10.1021/acsomega.9b03387
ACS Omega 2020, 5, 2254−2259

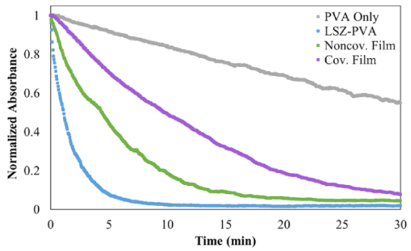

	LSZ-PVA Film	Cov. PVA Film	Noncov. PVA Film
Linear cell death slope	0.64	0.05	0.37
Specific activity (active units/mg LSZ)	2280	1440	1850
LSZ activity maintained (%)	100	63	81

Figure 4. Turbidimetric assays with films prepared with PVA as well as a table showing initial cell death slope, specific activity, and percentage of LSZ activity maintained for each film.

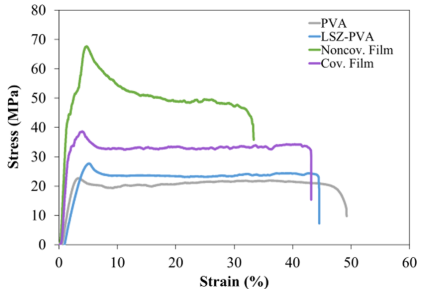

Component	Noncov. Film	Cov. Film	LSZ
SWNT	4 %	1 %	0 %
LSZ	25 %	2 %	24 %
PVA	71 %	97 %	76 %

Figure 5. Tensile testing data for films prepared with PVA as well as a table listing the composition by the mass fraction of components.

Table 2. Summary of Mechanical Testing Results Consisting of at Least Three Tests of Each Film Type with Standard Deviations

film	Young's modulus (MPa)	yield strength (MPa)	yield strain (%)	tensile strength (MPa)	max. strain (%)	toughness (MJ/m^3)
PVA	1030 ± 230	24 ± 8.8	4.7 ± 1.1	21 ± 4.2	44 ± 3.4	8.1 ± 3.1
LSZ−PVA	1120 ± 170	34 ± 5.2	5.0 ± 0.98	27 ± 3.5	34 ± 8.5	9.1 ± 2.6
noncov. PVA	4190 ± 360	75 ± 12	4.9 ± 0.60	48 ± 3.6	28 ± 8.9	13 ± 4.6
cov. PVA	2580 ± 310	39 ± 1.9	4.5 ± 0.46	33 ± 2.1	43 ± 0.50	13 ± 1.6

the SWNT increased LSZ activity based on active units/mg of LSZ.[19] This could be because Merli et al. considered CFU counts and not initial kinetics, differences in LSZ conformation due to the different nanotube diameters, or differences in nanotube surface chemistry.

Comparison of LSZ−SWNT−PVA Composite Film Properties. Nyankima et al.[17] showed that transparent and mechanically robust antimicrobial cast films could be made from combining of LSZ−SWNT dispersions with a PVA solution. Their work demonstrated that casting films from supernatant dispersions resulted in greater transparency, antimicrobial activity, and mechanical properties than casting films from the initial mixtures, which contained bundles and aggregates. However, their work did not explore the effects of covalent functionalization. Figure 4 shows assays performed with SWNT−LSZ−PVA, as well as control LSZ−PVA and PVA films. The PVA-only film showed some decreased absorbance; this was possibly due to some cellular aggregation from depletion attraction caused by the dissolution of PVA.[24] For each functionalization type, both the film and dispersion assays exhibited similar LSZ activity retention. The LSZ−PVA film showed higher activity than any of the SWNT−LSZ−PVA films. The noncovalent and covalent films both showed comparable specific activity to the dispersions 81 and 63% for the films, respectively, versus 80 and 66% for the dispersions, respectively. However, a significant observation was made over the course of the assays that the noncovalent films were more resistant to dissolution over the assay period; they remained intact, while the LSZ, PVA, and covalent LSZ−SWNT films dissolved completely.

Finally, as shown in Figure 5 and Table 2, tensile testing showed that dry LSZ−SWNT films had significantly higher Young's moduli than PVA and LSZ−PVA films. The noncovalent LSZ−SWNT−PVA films also had significantly higher yield and tensile strengths; these results are similar to those obtained by Nyankima et al.[17] The noncovalent films' Young's modulus, yield strength, and tensile strength were approximately 1.5 times higher than the covalent films. The covalent LSZ−SWNT−PVA films had similar yield and tensile strengths to the control films; this may be due to the lower concentration of SWNT. Interestingly, the toughness values were similar for all films.

CONCLUSIONS

There has been growing interest in stable carbon nanotube conjugates with functional biomaterials such as enzymes or biomarkers. The antibacterial enzyme, lysozyme, has been the focus of much attention because of its intrinsic antimicrobial properties and commercial availability. Favorable $\pi-\pi$ interactions between SWNT and LSZ's tryptophan residue enable facile noncovalent functionalization. In addition, covalent attachment can be readily achieved using EDC−NHS, a standard biochemical functionalization scheme. This work compared the properties of dispersions and films resulting from each of these approaches. Each method resulted in different relative concentrations; this, combined with the different nature of attachment, affected both dispersion and film properties. Covalent functionalization led to improved dispersion stability and longer duration of bacterial lysis

https://dx.doi.org/10.1021/acsomega.9b03387
ACS Omega 2020, 5, 2254−2259

relative to noncovalent LSZ−SWNT. Films prepared with LSZ−SWNT dispersions maintained similar LSZ activity to their dispersions. The presence of SWNT significantly increased films' Young modulus, but only the noncovalent films had significantly greater yield and tensile strengths. In addition, only the noncovalently functionalized films had significant hydrolytic stability during immersion in an aqueous solution. More research is needed to determine if this was solely due to the relative concentrations resulting from the two methods or if the nature of attachment also played a significant role. The results of this research show that both the noncovalent and covalent functionalization methods have merit. The choice of the method and composite concentrations should be based on the relative importance of dispersion stability, dispersion activity duration, hydrolytic stability, and film mechanical properties.

MATERIALS AND METHODS

The SWNT used in this study was CG200 (Lot # 14) obtained from Southwest Nano Technologies Inc (now CHASM, Norman, OK). SWNT composition determined by TGA showed 93% carbon content (85% pure SWNT; the rest was the catalyst). Lyophilized lysozyme from chicken egg white (Lot # 061M1329V) was purchased as a powder from Sigma-Aldrich (St. Louis, MO). PVA was purchased from Sigma-Aldrich with an average molecular weight of 195 000 g/mol and used as received.

Noncovalent dispersions were prepared by mixing 0.5 wt % lysozyme with deionized (DI) water for 5 min. Then, 0.1 wt % SWNT was added. The resulting dispersion was tip-sonicated for 30 min in an ice bath with pulses set to 5 s on 2 s off at 60% amplitude. Covalent attachment of lysozyme onto SWNT was performed using the procedure described by Merli et al. for LSZ attachment to MWNT.[19] In short, SWNT were acid oxidized in a 3:1 v/v sulfuric acid to the nitric acid mixture followed by thorough DI water rinsing. Carbodiimide activation of the carboxylic group was achieved in the presence of *N*-ethyl-*N*-(3-dimethylamino-propyl) carbodiimide hydrochloride (EDC) and *N*-hydroxysuccinimide (NHS), both purchased from Sigma-Aldrich. The resulting samples were rinsed thoroughly with 2-(*N*-morpholino)ethanesulfonic acid (MES) buffer (50 mM, pH 6.2). An LSZ solution (10 mg/mL, 10 mM phosphate buffer, pH 8) was then added to the activated and rinsed SWNT. This was tip-sonicated for 1 min and then allowed to react overnight on an orbital mixer. The mixture was washed to remove excess LSZ, lyophilized, and ground into a powder. The powder was added to water to achieve a concentration of 1 wt % powder and tip-sonicated for 30 min in an ice bath with pulses set to 5 s on 2 s off at 60% amplitude.

For both the noncovalent and covalent methods, the initial mixtures and the supernatants obtained after centrifugation were characterized. To determine if free (unbound) lysozyme was present, each type of sample was rinsed with successive 100 mL washes under vacuum filtration until no LSZ was detectable by UV−vis. The mixtures were centrifuged at 17 000*g* for 3 h to remove bundles, and the supernatants were characterized and retained. The supernatants were used for the antimicrobial assays and preparation of poly(vinyl alcohol) nanocomposite films.

Thermogravimetric analysis (TGA) was performed on TA Instruments Q5000 and Q50 TGAs to find the amounts of LSZ and SWNT present. FTIR was performed on the covalent and noncovalent supernatants, SWNT (as received) and native LSZ with a Nicolet FTIR instrument using attenuated total reflectance (ATR) with a germanium crystal. Raman spectra were obtained using a Renishaw inVia Raman microscope (Hoffman Estates, IL) with 514 and 785 nm lasers to characterize the degree of functionalization of the SWNT. The concentrations in the supernatant were determined by UV−vis spectroscopy and TGA. The amount of bound LSZ in the noncovalent dispersions was determined by successive washes with DI water and then using a combination of UV−vis spectroscopy to determine free LSZ concentration in the filtrate and a mass balance to determine the bound LSZ concentration, based on previously reported methods.[8,16,17]

A Thermo Scientific NanoDrop 2000c UV−vis spectrophotometer was used to determine LSZ and SWNT concentrations based on Beer−Lambert plots obtained at 280 and 660 nm, respectively. UV−vis was also used to measure LSZ activity based on the time-dependent decrease in turbidity on bacterial lysis of *M. lysodeikticus* (Sigma-Aldrich) in accordance with the method of Shugar et al.[22,25] A 0.015% w/v *M. lysodeikticus* (Sigma-Aldrich) bacterial suspension was prepared in a 66 mM potassium phosphate monobasic buffer (pH 6.24 adjusted by 1 M potassium hydroxide). A 10 mm path length quartz cuvette with 2.5 mL of the bacterial and 0.1 mL of sample dispersion or the diluted sample was subjected to a kinetic scan for 25 min at 450 nm. Normalized absorbances were obtained by dividing all data points by the initial absorbance. The concentration of dispersions was also obtained by a combination of UV−vis calibration curves and thermogravimetric analysis.

SWNT−LSZ−PVA films were prepared by adding a 5 wt % PVA solution to the dispersion to obtain 1.1 wt % PVA in each dispersion. 10 mL of SWNT−LSZ−PVA was placed in a 50 mm diameter glass dish and allowed to evaporate on an orbital shaker overnight to obtain a thin film. Assays were performed by the procedure stated above, adjusting the time to 30 min and placing a sample of the film with 50 mm^2 surface area into the bacterial suspension in place of dispersion. Tensile testing was performed with a 3 mm × 15 mm film sample on an Instron model 5500 with a 100 N load cell and with a crosshead speed of 1 mm/min.

AUTHOR INFORMATION

Corresponding Author

Virginia A. Davis − *Department of Chemical Engineering, Auburn University, Auburn, Alabama 36849, United States;* orcid.org/0000-0003-3126-3893; Email: davisva@auburn.edu

Authors

Matthew M. Noor − *Department of Chemical Engineering, Auburn University, Auburn, Alabama 36849, United States*

Joyanta Goswami − *Department of Chemical Engineering, Auburn University, Auburn, Alabama 36849, United States*

Complete contact information is available at: https://pubs.acs.org/10.1021/acsomega.9b03387

Notes

The authors declare no competing financial interest.

https://dx.doi.org/10.1021/acsomega.9b03387
ACS Omega 2020, 5, 2254−2259

■ ACKNOWLEDGMENTS

The authors would like to acknowledge funding from the Department of Education GAANN P200A150074 and the Auburn University Internal Grants Program.

■ REFERENCES

(1) Trozzi, F.; Marforio, T. D.; Bottoni, A.; Zerbetto, F.; Calvaresi, M. Engineering the fullerene-protein interface by computational design: The sum is more than its parts. *Isr. J. Chem.* **2017**, *57*, 547−552.
(2) Calvaresi, M.; Zerbetto, F. The devil and holy water: Protein and carbon nanotube hybrids. *Acc. Chem. Res.* **2013**, *46*, 2454−2463.
(3) Vaitheeswaran, S.; Garcia, A. E. Protein stability at a carbon nanotube interface. *J. Chem. Phys.* **2011**, *134*, No. 125101.
(4) Raffaini, G.; Ganazzoli, F. Protein adsorption on biomaterial and nanomaterial surfaces: A molecular modeling approach to study non-covalent interactions. *J. Appl. Biomater. Biomech.* **2010**, *8*, 135−145.
(5) Liang, F.; Chen, B. A review on biomedical applications of single-walled carbon nanotubes. *Curr. Med. Chem.* **2010**, *17*, 10−24.
(6) Nepal, D.; Geckeler, K. E. Proteins and carbon nanotubes: Close encounter in water. *Small* **2007**, *3*, 1259−1265.
(7) Asuri, P.; Bale, S. S.; Pangule, R. C.; Shah, D. A.; Kane, R. S.; Dordick, J. S. Structure, function, and stability of enzymes covalently attached to single-walled carbon nanotubes. *Langmuir* **2007**, *23*, 12318−12321.
(8) Horn, D. W.; Tracy, K.; Easley, C. J.; Davis, V. A. Lysozyme dispersed single-walled carbon nanotubes: Interaction and activity. *J. Phys. Chem. C* **2012**, *116*, 10341−10348.
(9) Nepal, D.; Balasubramanian, S.; Simonian, A. L.; Davis, V. A. Strong antimicrobial coatings: Single-walled carbon nanotubes armored with biopolymers. *Nano Lett.* **2008**, *8*, 1896−1901.
(10) Antonucci, A.; Kupis-Rozmysłowicz, J.; Boghossian, A. A. Noncovalent protein and peptide functionalization of single-walled carbon nanotubes for biodelivery and optical sensing applications. *ACS Appl. Mater. Interfaces* **2017**, *9*, 11321−11331.
(11) Di Giosia, M.; Valle, F.; Cantelli, A.; Bottoni, A.; Zerbetto, F.; Fasoli, E.; Calvaresi, M. Identification and preparation of stable water dispersions of protein - carbon nanotube hybrids and efficient design of new functional materials. *Carbon* **2019**, *147*, 70−82.
(12) Calvaresi, M.; Hoefinger, S.; Zerbetto, F. Probing the structure of lysozyme−carbon-nanotube hybrids with molecular dynamics. *Chem. - Eur. J.* **2012**, *18*, 4308−4313.
(13) Yang, F.; Liu, Y.; Gao, L.; Sun, J. Ph-sensitive highly dispersed reduced graphene oxide solution using lysozyme via an in situ reduction method. *J. Phys. Chem. C* **2010**, *114*, 22085−22091.
(14) Siepi, M.; Politi, J.; Dardano, P.; Amoresano, A.; De Stefano, L.; Maria Monti, D.; Notomista, E. Modified denatured lysozyme effectively solubilizes fullerene C60 nanoparticles in water. *Nanotechnology* **2017**, *28*, No. 335601.
(15) Calvaresi, M.; Zerbetto, F. Baiting proteins with c60. *ACS Nano* **2010**, *4*, 2283−2299.
(16) Horn, D. W.; Ao, G.; Maugey, M.; Zakri, C.; Poulin, P.; Davis, V. A. Dispersion state and fiber toughness: Antibacterial lysozyme-single walled carbon nanotubes. *Adv. Funct. Mater.* **2013**, 6082−6090.
(17) Nyankima, A. G.; Horn, D. W.; Davis, V. A. Free-standing films from aqueous dispersions of lysozyme, single-walled carbon nanotubes, and polyvinyl alcohol. *ACS Macro Lett.* **2014**, *3*, 77−79.
(18) Nie, H.; Wang, H.; Cao, A.; Shi, Z.; Yang, S.-T.; Yuan, Y.; Liu, Y. Diameter-selective dispersion of double-walled carbon nanotubes by lysozyme. *Nanoscale* **2011**, *3*, 970−973.
(19) Merli, D.; Ugonino, M.; Profumo, A.; Fagnoni, M.; Quartarone, E.; Mustarelli, P.; Visai, L.; Grandi, M. S.; Galinetto, P.; Canton, P. Increasing the antibacterial effect of lysozyme by immobilization on multi-walled carbon nanotubes. *J. Nanosci. Nanotechnol.* **2011**, *11*, 3100−3106.
(20) Dresselhaus, M. S.; Dresselhaus, G.; Saito, R.; Jorio, A. Raman spectroscopy of carbon nanotubes. *Phys. Rep.* **2005**, *409*, 47−99.
(21) Barth, A. Infrared spectroscopy of proteins. *Biochim. Biophys. Acta, Bioenerg.* **2007**, *1767*, 1073−1101.
(22) Sigma-Aldrich. Enzymatic Activity of Lysozyme (ec 3.2.1.17) http://www.sigmaaldrich.com/technical-documents/protocols/biology/enzymatic-assay-of-lysozyme.html.
(23) Nepal, D.; Balasubramanian, S.; Simonian, A. L.; Davis, V. A. Strong antimicrobial coatings: Single-walled carbon nanotubes armored with biopolymers. *Nano Lett.* **2008**, *8*, 1896−1901.
(24) Marenduzzo, D.; Finan, K.; Cook, P. R. The depletion attraction: An underappreciated force driving cellular organization. *J. Cell Biol.* **2006**, *175*, 681−686.
(25) Shugar, D. The measurement of lysozyme activity and the ultra-violet inactivation of lysozyme. *Biochim. Biophys. Acta* **1952**, *8*, 302−309.

https://dx.doi.org/10.1021/acsomega.9b03387
ACS Omega 2020, 5, 2254−2259